Thrombosis Research 133 (2014) 900–907

Contents lists available at ScienceDirect

Thrombosis Research

journal homepage: www.elsevier.com/locate/thromres

Regular Article

Biodistribution of the recombinant fusion protein linking coagulation factor IX with albumin (rIX-FP) in rats☆

Eva Herzog [a,*], Stephen Harris [b], Claire Henson [b], Andrew McEwen [b], Sabrina Schenk [a], Marc W. Nolte [a], Ingo Pragst [a], Gerhard Dickneite [a], Stefan Schulte [a], Sabine Zollner [a]

[a] CSL Behring GmbH, Preclinical Research and Development, 35041 Marburg, Germany
[b] Quotient Bioresearch Metabolic Chemistry, Rushden, UK

ARTICLE INFO

Article history:
Received 15 November 2013
Received in revised form 22 January 2014
Accepted 13 February 2014
Available online 22 February 2014

Keywords:
Albumin fusion
Biodistribution
Coagulation factor IX
Pharmacokinetics
Recombinant factor IX

ABSTRACT

Introduction: The recombinant fusion protein linking coagulation factor IX with albumin (rIX-FP) is undergoing clinical trials for prophylaxis and on-demand treatment of haemophilia B patients. The aim of this study was to investigate the pharmacokinetics, whole-body and knee joint distribution of rIX-FP following intravenous administration to rats, compared with a marketed, non-fused rFIX and recombinant human albumin.
Material and Methods: [^{3}H]-rIX-FP, [^{3}H]-rFIX or [^{3}H]-albumin were administered to rats followed by quantitative whole-body autoradiography over 24 or 240 hours, and the tissue distribution as well as elimination of radioactivity were measured.
Results: Elimination of all radioactivity derived from the three proteins was shown to occur primarily via the urine. The tissue distribution of [^{3}H]-rIX-FP and [^{3}H]-rFIX (but not of [^{3}H]-albumin) was comparable, both penetrating predominantly into bone, and well-perfused tissues, suggesting that the rIX moiety determines the distribution pattern of rIX-FP, while the albumin moity is responsible for the prolonged plasma and tissue retention. Detailed knee-joint analysis indicated rapid presence of [^{3}H]-rIX-FP and [^{3}H]-rFIX in synovial and mineralised bone tissue, mostly localised to the zone of calcified cartilage. Longest retention times were observed in the bone marrow and the endosteum of long bones. Intriguingly, [^{3}H]-rIX-FP- and [^{3}H]-albumin-derived radioactive signals were detectable up to 240 hours, while [^{3}H]-rFIX-derived radioactivity rapidly declined after 1 hour post-dosing correlating to the extended plasma half-life of [^{3}H]-rIX-FP.
Conclusion: The prolonged plasma and tissue retention of rIX-FP achieved by albumin fusion may allow a reduction in dosing frequency leading to increased therapeutic compliance and convenience.

Introduction

Factor IX (FIX) is the zymogen of a serine protease that circulates in plasma at an average concentration of 5 μg/ml [1]. Activated FIX (FIXa) is an integral part of the tenase enzyme complex activating factor X, ultimately leading to blood coagulation [2,3]. FIX-replacement therapy, using recombinant (rFIX) or plasma-derived (pdFIX) FIX is a safe and efficacious treatment approach to reduce bleeding rates among haemophilia B patients, while limiting haemarthrosis and arthropathy (potential causes of disability) [4]. Unfortunately, the relatively short terminal half-life of FIX of approximately 18–34 hours, necessitates frequent infusions every 2 or 3 days to maintain FIX clotting activity above 1% and to prevent spontaneous bleeding [5,6].

To improve therapeutic compliance and convenience, a novel recombinant fusion protein linking coagulation factor IX with albumin via a cleavable peptide linker (rIX-FP) has been designed to prolong the circulation time of FIX significantly; thus, improving its pharmacokinetic profile while maintaining its efficacy [7–9]. Understanding the tissue distribution of this novel coagulation factor construct is important to ensure that it reaches those areas necessary for maximum haemostatic efficacy. However, there is limited information available on the tissue distribution of FIX (rFIX/pdFIX) following intravenous administration and how fusion with albumin, as in the case of rIX-FP, may affect it. Therefore, this study aimed to investigate the pharmacokinetics and whole-body distribution of rIX-FP following intravenous administration of radiolabeled rIX-FP to rats, compared with a marketed, non-fused rFIX and recombinant human albumin, with particular focus on the bone–joint distribution profile.

Abbreviations: FIX, factor IX; FIXa, activated FIX; rFIX, recombinant FIX; pdFIX, plasma-derived FIX; rIX-FP, recombinant fusion protein linking factor IX with albumin; QWBA, quantitative whole-body autoradiography; LSC, liquid scintillation counting; LMW, low-molecular-weight; ATIII, antithrombin III; FcRn, neonatal Fc-receptor.

☆ Data partly presented at: XXIV Congress of the International Society of Thrombosis and Haemostasis, the Netherlands, 2013.

* Corresponding author at: CSL Behring GmbH, Emil-von-Behring-Str. 76, 35041 Marburg, Germany. Tel.: +49 6421 39 6106; fax: +49 6421 39 4663.
E-mail address: eva.herzog@cslbehring.com (E. Herzog).

http://dx.doi.org/10.1016/j.thromres.2014.02.010

Material and Methods

Radiolabelling and Characterisation of rIX-FP and rFIX

rIX-FP (CSL Behring GmbH, Germany), rFIX (BeneFIX®, Pfizer Pharma GmbH, Berlin, Germany) or albumin (Recombumin®, Novozymes Biopharma, Bagsvaerd, Denmark) were radiolabeled with N-succinimidyl-[2,3-^{3}H]-propionate (Quotient Bioresearch, Cardiff, UK), using the method described by Müller [10].

Treatments

Male Sprague-Dawley rats (Charles River, UK) received a slow bolus radioactive dose of 11−16 MBq/kg (320−420 μCi/kg) [^{3}H]-rIX-FP, [^{3}H]-rFIX, or [^{3}H]-albumin. All animals received care in compliance with the European Convention on Animal Care and the study was approved by the local Ethics Committee.

Plasma Analysis

Following intravenous dosing, blood samples (~5−10 ml) were collected into individual heparinised containers using cardiac puncture under anaesthesia (isofluorane) at the following post-dose time points (one animal/time point): 0.25, 1, 3, 8, 24, 72, 120, and 240 hours for [^{3}H]-rIX-FP- and [^{3}H]-albumin-treated animals, and based on previous pharmacokinetic data, 0.25, 1, 3, and 24 hours for [^{3}H]-rFIX-treated animals. The whole-blood samples were centrifuged and the resultant plasma harvested.

Excretion Balance

After dosing, animals selected for the final autoradiography time point (240 hours for [^{3}H]-rIX-FP or [^{3}H]-albumin, and 24 hours for [^{3}H]-rFIX) were returned to glass metabolism cages for separate urine (at 0−8 hours, 8−24 hours and 24-hour intervals thereafter) and faeces (at 24-hour intervals) collection. At the end of the observation period, the metabolism cages were rinsed with water followed by methanol, and the washings collected for quantitative radiochemical analysis.

Quantitative Whole-body Autoradiography (QWBA)

QWBA analysis was performed based on the technique of Ullberg [11] at time points up to 24 ([^{3}H]-rFIX) or 240 hours ([^{3}H]-rIX-FP, [^{3}H]-albumin). Sagittal sections of the body were assessed at up to five different levels: Level 1, exorbital lachrymal gland; Level 2, intra-orbital lachrymal gland; Level 3, harderian gland/adrenal gland; Level 4, thyroid gland; and Level 5, brain and spinal cord. A calibration curve was created via SeeScan using data from the ^{3}H-blood standards from which tissue concentrations of radioactivity were determined (nCi/g). Percentage total dose/tissue was also determined. Additionally, one hind limb from each animal was used for separate sectioning and a more detailed analysis of the knee joint.

Quantitative Radiochemical and Chromatographic Analysis

Liquid scintillation counting (LSC) was used to determine the radioactivity level (disintegrations/minute) of the dose formulation, plasma, urine, faeces, and cage wash using a Packard 2300TR liquid scintillation analyser (PerkinElmer, Waltham, MA, USA) with automatic external standard quench correction and Ultima Gold XR scintillation fluid (PerkinElmer). Proportions of radioactivity in purified ^{3}H-labeled protein solutions, plasma and urine samples were determined by high-performance liquid chromatography (HPLC; Agilent 1100 HPLC system with ultraviolet detection at 280 nm) using a Phenomenex BIOSEP SEC 2000 size exclusion column (300 × 7.8 mm; mobile phase 100 mM sodium phosphate or 0.1 M phosphate buffer for protein solutions and body fluids, respectively). FIX antigen levels were also measured to confirm the presence of rIX-FP in tissues.

Results

Characterisation of [^{3}H]-rIX-FP and [^{3}H]-rFIX Preparations

Radiochemical purity of the [^{3}H]-rIX-FP, [^{3}H]-rFIX, and [^{3}H]-albumin formulations was > 90% as determined by HPLC analysis and shown in Fig. S1a i, ii, and iii, respectively. Assessment of the biological activity confirmed that 100% of rIX-FP specific activity was maintained following [^{3}H]-labelling based on measurements of FIX activity (Fig. S1b).

Analysis of Circulating Radioactivity and Pharmacokinetics

Plasma analysis confirmed the mean dose levels of ~400 μCi/kg in each treatment group: [^{3}H]-rIX-FP, 409 μCi/kg; [^{3}H]-rFIX, 425 μCi/kg; and [^{3}H]-albumin, 382 μCi/kg. For direct comparisons of FIX products, radioactive dose level differences were considered when interpreting the plasma and tissue concentration data. Plasma radioactivity levels and representative radiochromatograms of [^{3}H]-rIX-FP, [^{3}H]-rFIX, and [^{3}H]-albumin are shown in Table S1 and Fig. S2 (a-c), respectively. Levels of intact protein recovered in plasma are shown in Table 1 and Fig. 1a.

[^{3}H]-rIX-FP

Unchanged [^{3}H]-rIX-FP (peak at ~7 minutes) was the major component in plasma, accounting for ~100% of all radioactivity up to 8 hours post-dosing (see Table 1). At 24 hours, this declined to 73.0%, with the remaining radioactivity composed of two peaks that co-chromatographed with albumin (at ~8.5 minutes) and a low-molecular-weight (LMW) component (at 13.4 minutes), and represented 16.5% and 3.7% of the total radioactivity, respectively (Table S1 and Fig. S2a). [^{3}H]-rIX-FP levels continued to decline with time, with < 1.0% at 120 hours and almost undetectable at 240 hours (Table 1).

Table 1
Recovery* of radioactivity in rat plasma, urine, and faeces following a single intravenous administration of [^{3}H]-rIX-FP, [^{3}H]-rFIX, or [^{3}H]-albumin.

Sample	Time (hours)	[^{3}H]-rIX-FP	[^{3}H]-rFIX	[^{3}H]-albumin
Plasma	0.25	100	91.7	100
	1	100	86.3	100
	3	100	68.6	98.3
	8	100	–	96.3
	24	73.0	44.3	97.4
	72	60.7	–	79.3
	120	0.97	–	73.6
	240	0.29	–	BLQ
Urine	0–8	13.5	11.7	10.7
	8–24	26.4	39.3†	36.7
	24–48	16.9	–	28.7
	48–240	16.1	–	37.2
	Subtotal	72.9	51.0	113.3
Faeces	0–24	0.9	8.9	3.7
	24–48	0.8	–	1.9
	48–240	2.6	–	6.9
	Subtotal	4.3	8.9	12.5
Cage wash	**Subtotal**	3.7	2.9	0.7
Total		80.8	62.8	126.5

*Expressed as % of overall radioactivity administered. †Sample collection for rFIX was 0−6 hours. BLQ, below limit of quantification. rFIX, recombinant factor IX; rIX-FP, recombinant fusion protein linking coagulation factor IX with albumin; –, no measurement for that time point.

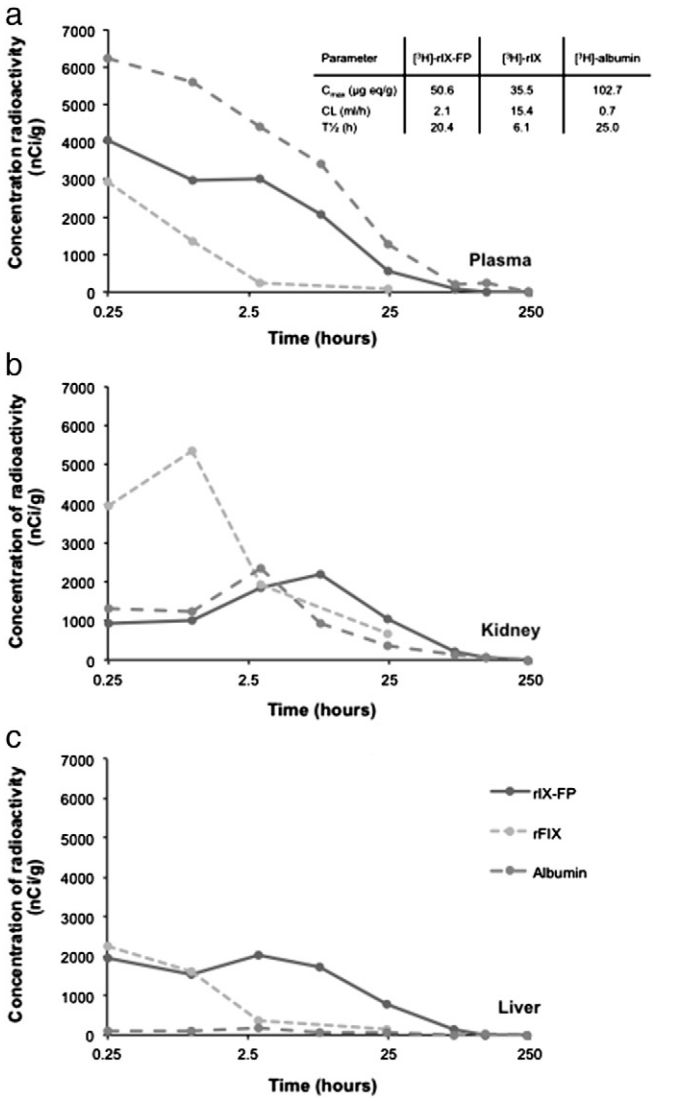

Fig. 1. Concentration of radioactivity in plasma (a), kidney (b), and liver (c) at 0.25–240 hours following intravenous administration of [^{3}H]-rIX-FP, [^{3}H]-rFIX, or [^{3}H]-albumin to rats. rFIX, recombinant factor IX; rIX-FP, recombinant fusion protein linking coagulation factor IX with albumin.

Pharmacokinetic analysis based on plasma levels obtained at 240 hours ([^{3}H]-rIX-FP; [^{3}H]-albumin) or 24 hours ([^{3}H]-rFIX) indicated that [^{3}H]-rIX-FP was cleared slowly with a terminal half-life of 20.4 hours and a clearance of 2.1 ml/hour (Fig. 1a).

[^{3}H]-rFIX

Unchanged [^{3}H]-rFIX in plasma at 15 minutes post-dose accounted for 91.7% of the total radioactivity (Table 1). This declined to 44.3% at 24 hours post-dose, with the majority of the remaining radioactivity (10.5%) associated with a LMW component (Table S1 and Fig. S2b). [^{3}H]-rFIX had a shorter half-life of 6.1 hours and a faster clearance of 15.4 ml/hour compared with [^{3}H]-rIX-FP (Fig. 1a).

[^{3}H]-albumin

[^{3}H]-albumin was detected in plasma as a single peak at ~8.5 minutes (Fig. S2c). Up to 3 hours, all radioactivity measured was attributed to intact protein (Table 1). From 8 to 240 hours, a second LMW peak appeared at 13 minutes (Table S1 and Fig. S2c). Similarly to [^{3}H]-rIX-FP, levels of [^{3}H]-albumin dropped to undetectable levels after 240 hours (Table 1). [^{3}H]-albumin had a half-life of 25.0 hours and a clearance of 0.7 ml/hour (Fig. 1a).

Excretion Balance

[^{3}H]-rIX-FP

Urinary excretion accounted for 72.9% of the [^{3}H]-rIX-FP dose eliminated up to 240 hours (Table 1). [^{3}H]-rIX-FP was eliminated in the form of a non-volatile LMW component, in the absence of any high-molecular-weight components (Fig. S2d). Faecal elimination accounted for 4.3% of the dose (Table 1). Overall, 80.9% of the total administered dose was recovered by 240 hours (Table 1).

[^{3}H]-rFIX

Up to 24 hours post-dose of [^{3}H]-rFIX, the majority of radioactivity was recovered in the urine (51.0%) in the form of a LMW component (Table 1 and Fig. S2e); 8.9% was eliminated via the faecal route (Table 1).

[^{3}H]-albumin

Urinary excretion accounted for almost half (47.5%) of the [^{3}H]-albumin elimination during the first 24 hours, with a total of 113.4% being recovered by 240 hours in the form of a LMW component (Table 1 and Fig. S2f); faecal excretion represented 12.5% of the dose (Table 1).

Tissue Distribution

Tissue Concentrations and Kinetics

[^{3}H]-rIX-FP. Fig. 2 and Fig. S3 display the quantitative whole boday autoradiography images obtained at two different sectioning levels at 0.25 to 24 hours post [^{3}H]-rIX-FP dosing. Image analysis confirmed that peak [^{3}H]-rIX-FP radioactivity levels were detected in the adrenal gland, followed by the kidney (particularly the medullary region), bone endosteum, spleen, lung, liver, and bone marrow (maximum concentrations of 2,020.0–7,040.0 nCi/g). High levels were also detected in other well-vascularised tissues such as the mucosa of the intestines, myocardium, and periodontal membrane (with maximum concentrations of 1,140.0—1,980.0 nCi/g), and the bulbo-urethral, pituitary glands, epididymis, and testes (maximum concentrations of 720.0—2,110.0 nCi/g).

Comparison of the tissue radioactivity over time indicated that peak radioactivity concentrations generally occurred at 3—8 hours post-dose, except in the adrenal gland and spleen, where they occurred at 0.25 hours and declined thereafter (Fig. 2 and Fig. S3). Levels in spleen, lung, and liver remained approximately constant at 0.25–8 hours post-dose. The longest radioactivity retention was in bone endosteum. Comparable levels were only detected up to 24 hours in other tissues (Fig. 2). Levels in the kidney, whose concentrations over time are illustrated in Fig. 1b, increased up to 8 hours post-dose, whereas concentrations in the liver remained steady up to 3 hours and decreased thereafter (Fig. 1c).

The timecourse of radioactivity concentrations observed along the gastrointestinal (GI) tract is listed in Table S2. As can be seen, peak concentrations of [^{3}H]-rIX-FP in the small (350.0 nCi/g) and large (69.2 nCi/g) intestines occurred at 3—8 hours, whereas the caecum level remained below the limit of quantification, indicating reabsorption or re-use of radiolabeled material during its GI passage.

In addition to autoradiographic tissue analysis, FIX antigen levels were determined in homogenized tissue samples following intravenous dosing of rIX-FP to rats. Preliminary data could confirm that the radioactive signals corresponded to the rIX-FP protein (Fig. S4).

[^{3}H]-rFIX. The pattern of tissue distribution of [^{3}H]-rFIX was identical to that of [^{3}H]-rIX-FP as can seen in Fig. 3 displaying QWBA images obtained at 0.25 hours and 24 hours post dosing (maximum concentrations of 1,630.0—6,240 nCi/g). At this later timepoint of 24 hours, highest levels occurred in the bone endosteum.

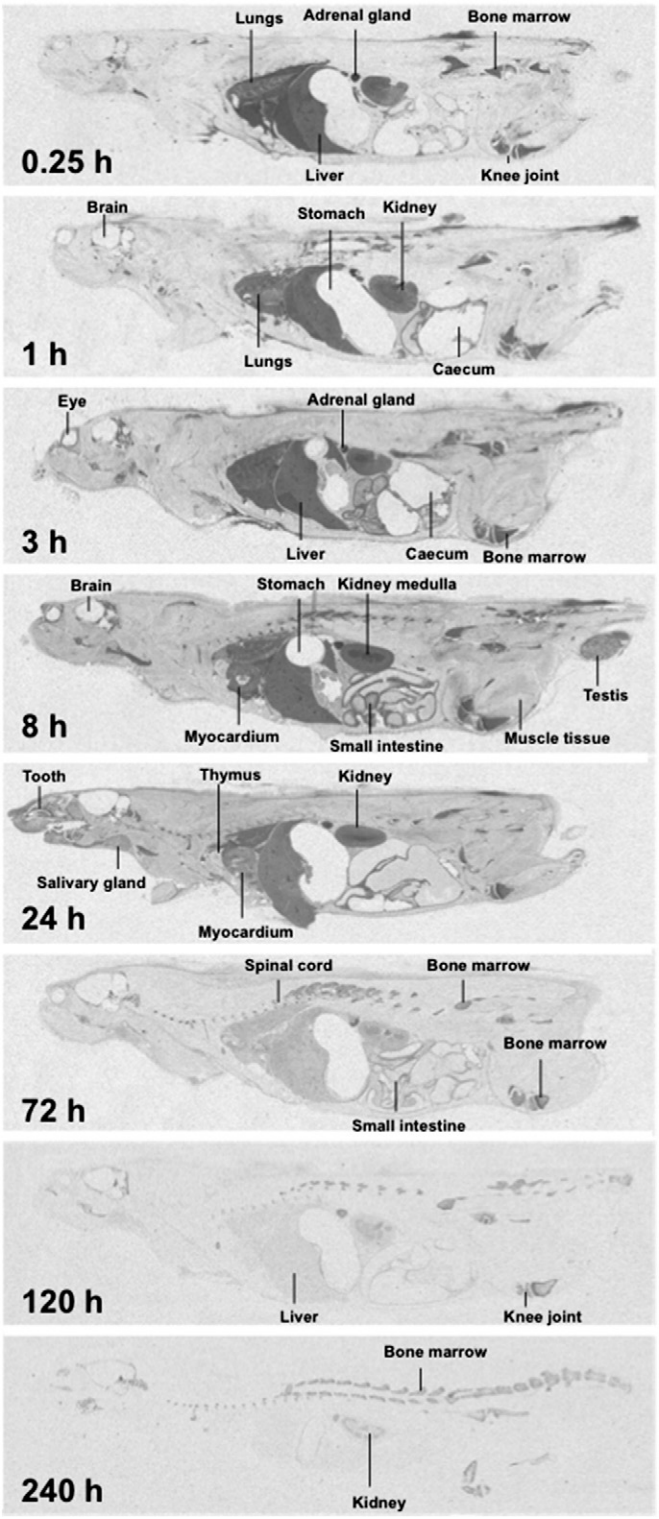

Fig. 2. Quantitative whole-body autoradiography images obtained at 0.25–240 hours following a single intravenous administration of [^{3}H]-rIX-FP to male albino rats (Level 3). h, hours; rFIX, recombinant factor IX; rIX-FP, recombinant fusion protein linking coagulation factor IX with albumin.

At the early time points, kidney concentrations of [^{3}H]-rFIX exceeded those of the liver by > 2-fold, confirming the kidney as the primary excretion organ of [^{3}H]-rFIX (Fig. 1b,c). Additionally, concentrations up to 5,870.0 nCi/g were detected in bladder contents, while concentrations within the small intestine, large intestine, and caecum contents remained < 178.0 nCi/g. However, in contrast to [^{3}H]-rIX-FP treatment, radioactivity was detectable within caecum contents, peaking at 128.0 nCi/g at 24 hours (Table S2).

[^{3}H]-albumin. In contrast to [^{3}H]-rIX-FP and [^{3}H]-rFIX, the highest tissue concentrations following [^{3}H]-albumin administration occurred in the periodontal membrane, tooth pulp, and bulbo-urethral gland (maximum levels 4,070.0—4,650.0 nCi/g); followed by the lungs, kidney, and bone endosteum (2,340.0—3,400.0 nCi/g) (Fig. 3). High radioactivity concentrations were also observed in other highly vascularised tissues [nasal and caecum mucosa, myocardium, stomach wall, aorta (1,230.0—1,930.0 nCi/g)], as well as the epididymis, testes, lymph nodes, harderian glands, and bone periosteum (1,040.0—1,530.0 nCi/g).

Following [^{3}H]-albumin treatment, maximum concentrations were generally reached at 3 hours post-dose. By 72 hours, radioactivity concentrations of all tissues had declined markedly with the longest tissue retention seen for the bone periosteum at 240 hours (data not shown). High levels of radioactivity were detected in the kidney, particularly the medulla region, which reached peak levels after 3 hours, slightly earlier than that of [^{3}H]-rIX-FP, but later than that of [^{3}H]-rFIX (Fig. 1b). Also, in contrast to [^{3}H]-rIX-FP and [^{3}H]-rFIX, concentrations of [^{3}H]-albumin-derived radioactivity in the liver remained <179.0 nCi/g, much lower than levels with [^{3}H]-rIX-FP or [^{3}H]-rFIX (Fig. 1c). Concentrations within small intestine contents reached a maximum of 492.0 nCi/g at 1 hour post-dose. In comparison, large intestine and caecum contents displayed maximum concentrations of only 52.3 and 96.7 nCi/g, respectively, again indicating some reabsorption of radioactivity (Table S2).

Total Dose Per Tissue

[^{3}H]-rIX-FP. In addition to the tissue concentrations of radioactivity, the total dose of radioactivity per tissue was determined and indicated that the liver received the highest total dose of [^{3}H]-rIX-FP, followed by muscle, kidney, lungs, and bone marrow (Fig. 4a).

[^{3}H]-rFIX. The pattern of the total radioactivity per tissue derived from [^{3}H]-rFIX was similar to that seen after [^{3}H]-rIX-FP dosing (Fig. 4b). However, at 24 hours post-dose, the levels of [^{3}H]-rFIX-derived radioactivity in most tissues had declined to levels below those seen with [^{3}H]-rIX-FP.

[^{3}H]-albumin. Muscle tissue received the highest total dose of [^{3}H]-albumin (Fig. 4c). Overall, 73.3% of the dose could be detected within muscle at 8 hours. Levels in muscle, intestinal mucosa, skin, and lymph nodes were higher at 24 than 0.25 hours.

Knee-joint Distribution

[^{3}H]-rIX-FP. Autoradiography images of the knee joint area analysed seperately are compared in Fig. 5. Fig. S5 includes the corresponding radioactivity concentrations determined for knee joint tissues. The data show that the highest radioactivity concentrations occurred in the calcified cartilage of the growth plate (5,190.0 nCi/g), followed by the bone endosteum (3,440.0 nCi/g), bone marrow (2,200.0 nCi/g), synovial space (709.0 nCi/g) and bone periosteum (515.0 nCi/g). Compact bone of the femur, fibula, and tibia, epiphysial plate and meniscus displayed low levels throughout. As can be seen in Fig. 5, maximum concentrations occurred at 8 hours, except in the periosteum, which peaked at 3 hours, and in the bone endosteum, which peaked at 120 hours and exhibited the longest retention of radioactivity.

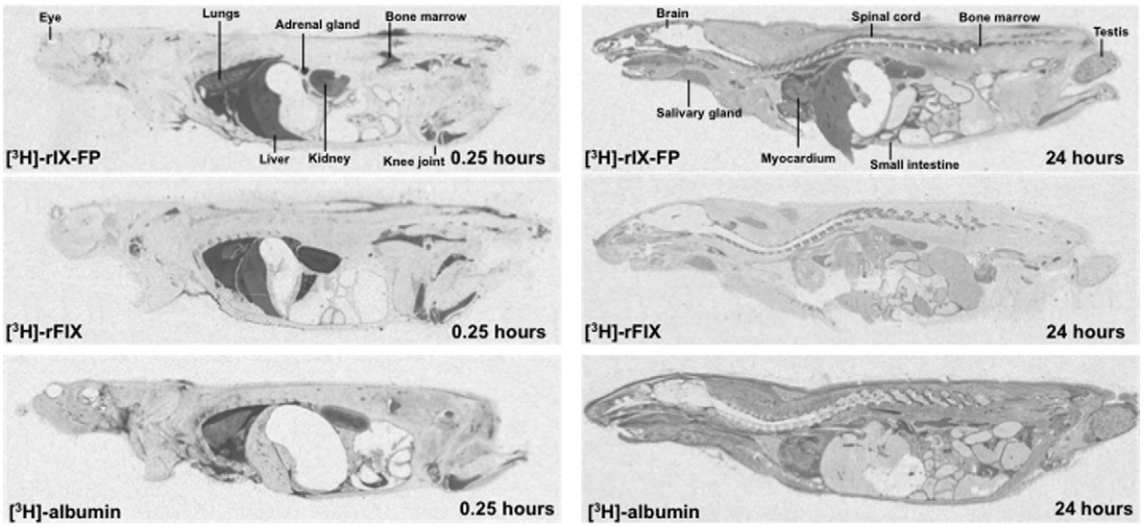

Fig. 3. Quantitative whole-body autoradiography image obtained at 0.25 (left panel) or 24 hours (right panel) after single intravenous administration of [^{3}H]-rIX-FP, [^{3}H]-rFIX, or [^{3}H]-rFIX to rats. rFIX, recombinant factor IX; rIX-FP, recombinant fusion protein linking coagulation factor IX with albumin.

[^{3}H]-rFIX. Peak [^{3}H]-rFIX concentrations in the knee joint were observed at ~1 hour post-dose, with a similar overall distribution profile to that of [^{3}H]-rIX-FP (Fig. 5 and Fig. S5). Highest concentrations also occurred in the calcified cartilage of the growth plate and endosteum, and low levels within compact bone or the synovial space. However, peak levels in calcified cartilage, endosteum, bone marrow, and periosteum (413.0—3,320.0 nCi/g), were below those seen following [^{3}H]-rIX-FP.

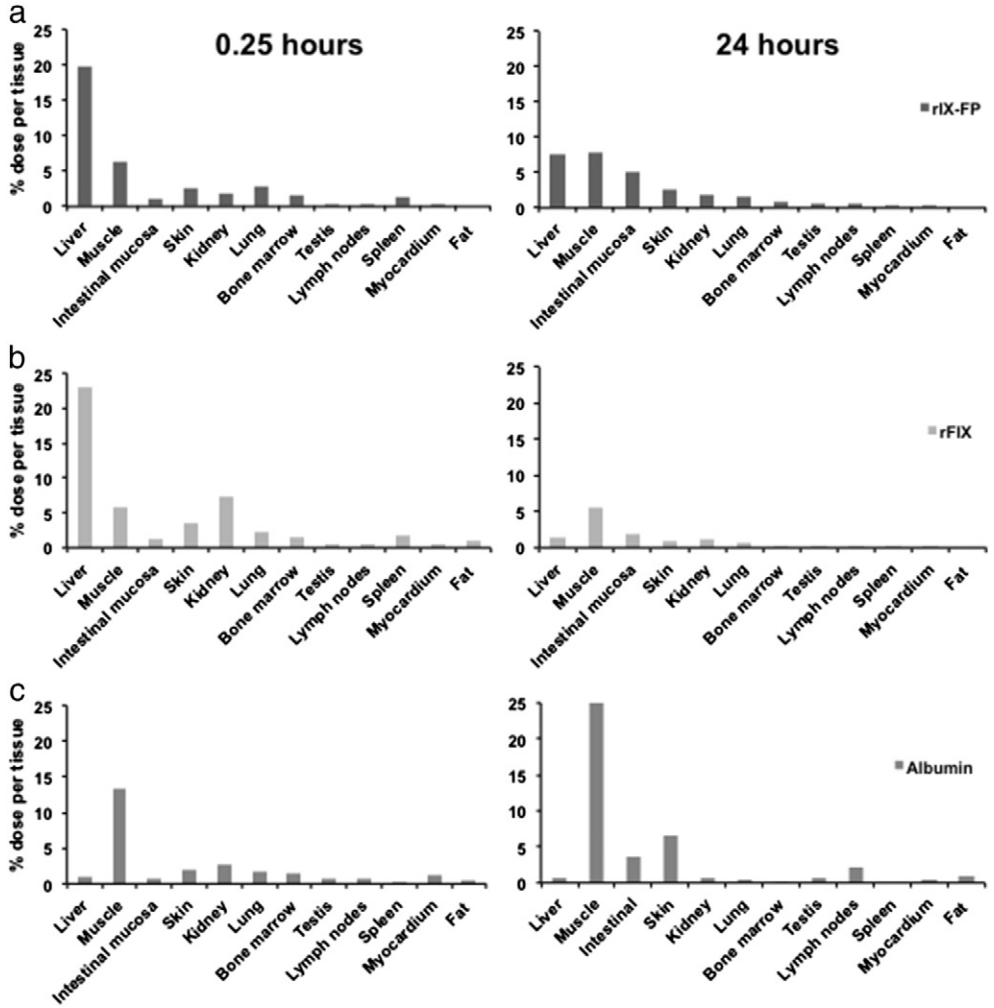

Fig. 4. Tissue distribution of radioactivity (average of % dose per tissue) at 0.25 and 24 hours following intravenous administration of [^{3}H]-rIX-FP (a), [^{3}H]-rFIX (b), or [^{3}H]-albumin (c) to rats. Tissue distribution cut-off: minimum of 0.5% per tissue at any given time point. rFIX, recombinant factor IX; rIX-FP, recombinant fusion protein linking coagulation factor IX with albumin.

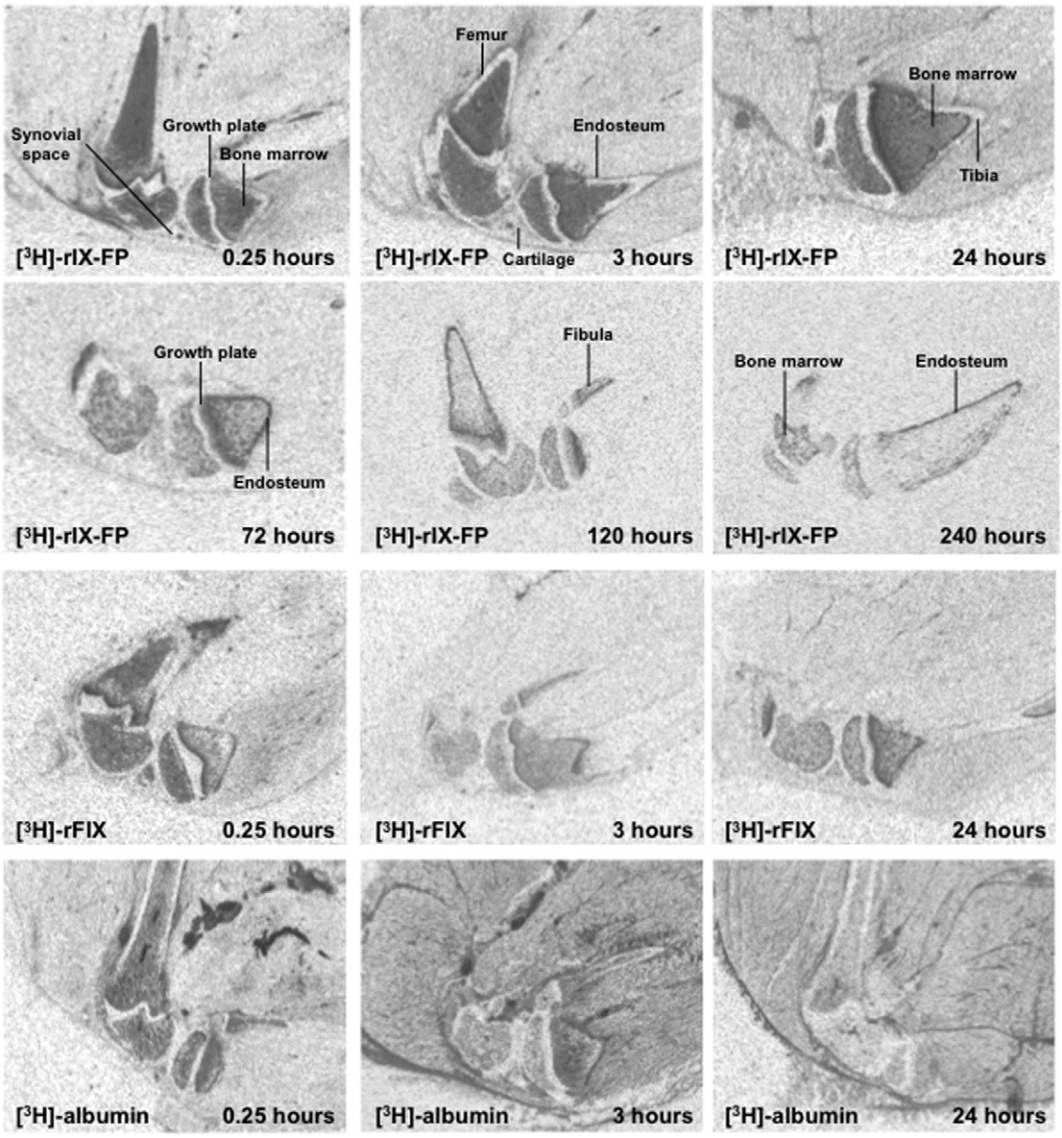

Fig. 5. Quantitative whole-body autoradiography images of knee-joint region following a single intravenous administration of [^{3}H]-rIX-FP, [^{3}H]-rFIX, or [^{3}H]-albumin to rats. rFIX, recombinant factor IX; rIX-FP, recombinant fusion protein linking coagulation factor IX with albumin.

[^{3}H]-albumin. Following [^{3}H]-albumin dosing, concentrations of radioactivity within the knee joint tissues were lower compared with [^{3}H]-rIX-FP and maximum levels were observed in the bone periosteum (2,570.0 nCi/g), with peak levels at 3 hours post-dose, followed by the calcified cartilage (1,590.0 nCi/g), bone endosteum (814.0 nCi/g), and bone marrow (576.0 nCi/g), which peaked at 0.25 hours post-dosing (Fig. 5and Fig. S5).

Discussion

This study aimed to define further the *in vivo* characteristics of rIX-FP, which is currently undergoing clinical trials. Direct comparison with a currently available rFIX product, which has been approved for clinical use since 1997 [12,13], enabled an investigation of the influence of albumin fusion on the tissue distribution profile of rFIX.

Plasma Kinetics and Elimination

Importantly, [^{3}H]-rIX-FP had a prolonged plasma terminal half-life compared with [^{3}H]-rFIX (20.4 versus 6.1 hours). This half-life extension is a key feature of rIX-FP and results from the fusion with albumin and agrees with studies by Metzner et al. [7] and Nolte et al. [8] showing an increase in the terminal half-life over rFIX by ~2.3- to 5.0-fold following albumin fusion across animal species. The former study furthermore confirms that the [^{3}H]-labelling procedure does not affect the pharmacokinetic characteristics of rIX-FP or rFIX as equal values for the terminal half-lives in rats were reported as seen in the present study (i.e. 24.1 versus 5.1 hours) [7].

The main elimination route for [^{3}H]-rIX-FP, [^{3}H]-rFIX, and [^{3}H]-albumin was renal, as indicated by the urinary versus faecal excretion profile and radioactivity concentrations within the kidney, and as described by previous studies of rFIX [14,15]. The majority of the radioactivity excreted in urine was in the form of a non-volatile LMW component, while intact rIX-FP, rFIX, or albumin proteins were absent, suggesting endocytosis of the proteins and subsequent degradation by lysosomal proteases, as described for other proteins [16,17].

Following administration of [^{3}H]-rIX-FP and [^{3}H]-rFIX, but not [^{3}H]-albumin, substantial radioactivity levels were detected within the liver, accounting for the highest total dose/tissue, indicating an important role of the liver during FIX metabolism and subsequent distribution. One explanation may be the interaction of FIX with thrombin-binding

sites, such as the serine protease inhibitor antithrombin III (ATIII), on endothelial cells of the liver [14,15] or specific low-density lipoprotein elimination pathways [18,19].

Similarly, following intravenous administration of [^{125}I]-FIXa or [^{131}I]-rFIX to rodents, 80 — 90% of the radioactivity was recovered in the liver at 2 — 5 minutes post-dose [14,15]. The same studies also reported accumulation of radioactivity in the kidneys.

The radioactivity levels in both the liver and kidney rapidly declined after [^{3}H]-rFIX dosing, which agrees with studies that reported no accumulation of mouse rFIX in these organs [20]. Similarly, there was no retention or accumulation of radioactivity following [^{3}H]-rIX-FP or [^{3}H]-albumin administration, even though the presence of albumin appeared to result in a delayed decrease in kidney and liver concentrations, with peak levels occurring at 3–8 hours.

Interestingly, a potential reabsorption of radioactive components during their passage through the gastrointestinal tract was observed, as indicated by the radioactivity levels in the small intestine and caecum contents, together with the high radioactivity levels in the intestinal mucosa, which would indicate enterohepatic circulation of [^{3}H]-rIX-FP and [^{3}H]-rFIX or their degradation products.

Tissue Distribution

Albumin fusion did not affect the tissue distribution profile of [^{3}H]-rIX-FP compared with [^{3}H]-rFIX. However, while initial radioactivity levels were comparable for both [^{3}H]-rIX-FP and [^{3}H]-rFIX, levels of [^{3}H]-rFIX declined much earlier, beginning 1 hour post-dose. In contrast, signals of [^{3}H]-rIX-FP were detectable until much later time points: up to 240 hours in bone tissue, adrenal gland, kidney, and intestinal mucosa. Although, at this time point, plasma radioactivity could not be directly assigned to intact [^{3}H]-rIX-FP protein, as the similarity in the distinct pattern of tissue distribution to all earlier time points suggests that the tissue concentration may still represent unchanged protein. Similar to [^{3}H]-rIX-FP, [^{3}H]-albumin-derived radioactivity was detectable up to 240 hours, indicating comparable tissue retention. However, in contrast to [^{3}H]-rIX-FP and [^{3}H]-rIX, [^{3}H]-albumin elicited a distinct tissue distribution pattern. Thus, it is concluded that rFIX is the main determinant of the tissue distribution of rIX-FP, whereas albumin fusion appears to determine its extended tissue retention.

Similar to studies by Chang et al., no radioactivity was observed in brain tissue [14], thereby limiting the prothrombotic risk associated with FIX within this tissue. Interestingly, initial distribution was particularly high for the adrenal gland, which seemed to be a specific property of [^{3}H]-rIX-FP and [^{3}H]-rFIX, as it was not observed for [^{3}H]-albumin. Glandular tissues (e.g., bulbo-urethral gland, epididymis, pituitary gland, salivary gland, thyroid, prostate, lachrymal or Harderian gland) showed elevated radioactivity levels following administration of all three proteins.

The high levels of radioactivity observed in well-vascularised tissues may be due to the high vascular concentrations of the test items potentially resulting in increased tissue compartmentalisation, and possibly incomplete perfusion of animals post-mortem. However, some degree of tissue compartmentalisation is likely for the FIX proteins studied. Several mechanisms have been proposed for the fate of coagulation proteins upon intravenous administration. The interaction of the FIX Gla domain with collagen IV on endothelial surfaces has been shown to affect the rate of FIX clearance and endothelial sequestration [21–23]. The endothelium may represent a FIX reservoir, protecting FIX from normal clearance mechanisms [24]; however, conflicting evidence exists on FIX binding to endothelial cells following systemic exposure [15,20].

Binding to the neonatal Fc-receptor (FcRn) may represent another mechanism directly affecting the biodistribution of rIX-FP and albumin, but not of rFIX [25–27], and underlying the prolonged biological half-life of rIX-FP. However, translation of FcRn effects from animal studies to humans is complicated due to species differences in FcRn binding [28,29]. In addition to FcRn, albumin interacts with other receptors and extracellular matrix components, which may affect the pharmacokinetics and biodistribution of the fused coagulation factor [30–33]. Further studies are warranted to investigate the exact interaction between rIX-FP and the endothelial cell lining to explore potential sequestration mechanisms to extravascular tissue.

In-depth analysis of the knee-joint distribution confirmed the longest retention period of [^{3}H]-rFIX and [^{3}H]-rIX-FP within the mineralised bone region, particularly the bone-formative areas [20]. Investigations from Thomsen and co-workers suggested that only proteins containing the Gla-domain are sequestered in bone via binding to hydroxyapatite during mineral maturation, with the bone compartment serving as a storage site for these vitamin K-dependent clotting factors [34]. While rFIX sequestered in the bone disappeared by 24 hours post-dose, [^{3}H]-rIX-FP could be detected up to 120 — 240 hours. This may be explained by the interaction of albumin with its receptors or other matrix components, such as osteonectin [35]. As osteonectin is localised to mineralised bone trabeculae and occurs at higher levels in the matrix than in bone cells, binding to osteonectin may partly explain the observed bone distribution and retention of rIX-FP. Furthermore, increased albumin permeability of the blood — joint barrier has been described for patients with rheumatoid arthritis [36], and in preclinical arthritis models [37]; thus, rIX-FP retention could be related to preferential uptake of albumin. Follow-up studies are required to confirm the presence of intact rIX-FP within bone tissue and further characterise the exact binding sites.

Overall, the present QWBA studies comparing the distribution and elimination of [^{3}H]-rIX-FP, [^{3}H]-rFIX, and [^{3}H]-albumin indicate that recombinant genetic fusion of rFIX to human albumin using a cleavable linker does not affect the general tissue distribution profile of rIX-FP compared with rFIX. However, albumin fusion markedly extends the circulatory half-life and tissue retention after intravenous administration. The prolonged tissue retention may be due to changes in specific receptor-mediated mechanisms, or albumin-mediated increase in molecular volume and masking of rFIX, rendering the protein less immunogenic and more resistant to proteases, ultimately resulting in retarded clearance [38,39]. However, the exact mechanism would still need to be elucidated and confirmed.

It should be noted that the present study was conducted in healthy rats which display normal FIX background levels in contrast to Hemophilia B patients. Future biodistribution studies using FIX-deficient animal models may therefore further support the translation of animal biodistribution data to human patients.

The favourable pharmacokinetic and pharmacodynamic profile of rIX-FP may directly translate into improved coagulation replacement therapy with less frequent dosing required to maintain appropriate FIX levels during prophylaxis, particularly within joint tissue.

Supplementary data to this article can be found online at http://dx.doi.org/10.1016/j.thromres.2014.02.010.

Conflicts of Interest Statement

EH, SZ, MWN, SSch, IP, GD and SS are employees of CSL Behring GmbH, Marburg, Germany. SH, CH and AM are employees of Quotient Bioresearch, Rushden, UK.

Acknowledgements

The authors would like to thank Elmar Raquet, Patrick Letmade, and Alan Lathall for their technical assistance, and Swiss Medical Press who received funding from CSL Behring for editorial assistance.

References

[1] Suzuki LA, Thompson AR. Factor IX antigen by a rapid staphylococcal protein A-membrane binding radioimmunoassay: results in haemophilia B patients and carriers and in fetal samples. Br J Haematol 1982;50:673–82.
[2] Osterud B, Bouma BN, Griffin JH. Human blood coagulation factor IX. Purification, properties, and mechanism of activation by activated factor XI. J Biol Chem 1978;253:5946–51.
[3] Jackson CM, Nemerson Y. Blood coagulation. Annu Rev Biochem 1980;49:765–811.
[4] Nilsson IM, Berntorp E, Lofqvist T, Pettersson H. Twenty-five years' experience of prophylactic treatment in severe haemophilia A and B. J Intern Med 1992;232:25–32.
[5] Björkman S, Shapiro AD, Berntorp E. Pharmacokinetics of recombinant factor IX in relation to age of the patient: implications for dosing in prophylaxis. Haemophilia 2001;7:133–9.
[6] Ewenstein BM, Joist JH, Shapiro AD, Hofstra TC, Leissinger CA, Seremetis SV, et al. Pharmacokinetic analysis of plasma-derived and recombinant F IX concentrates in previously treated patients with moderate or severe hemophilia B. Transfusion 2002;42:190–7.
[7] Metzner HJ, Weimer T, Kronthaler U, Lang W, Schulte S. Genetic fusion to albumin improves the pharmacokinetic properties of factor IX. Thromb Haemost 2009;102:634–44.
[8] Nolte MW, Nichols TC, Mueller-Cohrs J, Merricks EP, Pragst I, Zollner S, et al. Improved kinetics of rIX-FP, a recombinant fusion protein linking factor IX with albumin, in cynomolgus monkeys and hemophilia B dogs. J Thromb Haemost 2012;10:1591–9.
[9] Schulte S. Half-life extension through albumin fusion technologies. Thromb Res 2009;124(Suppl. 2):S6–8.
[10] Müller GH. Protein labeling with 3H-NSP (N-succinimidyl-[2,3,-3H]propionate). J Cell Sci 1980;43:319–28.
[11] Ullberg S. Studies on the distribution and fate of 35S-labelled benzylpenicillin in the body. Acta Radiol 1954(Suppl. 118):1–110.
[12] Kaufman RJ, Wasley LC, Furie BC, Furie B, Shoemaker CB. Expression, purification, and characterization of recombinant gamma-carboxylated factor IX synthesized in Chinese hamster ovary cells. J Biol Chem 1986;261:9622–8.
[13] BeneFIX [(Coagulation Factor IX (Recombinant)]. Available at: http://labeling.pfizer.com/showlabeling.aspx?id=492. [Accessed October 24, 2013].
[14] Chang C-H, Chou T-K, Yang C-Y, Chang T-J, Wu Y-H, Lee T-W. Biodistribution and pharmacokinetics of transgenic pig-produced recombinant human factor IX (rhFIX) in rats. In Vivo 2008;22:693–8.
[15] Fuchs HE, Trapp HG, Griffith MJ, Roberts HR, Pizzo SV. Regulation of factor IXa in vitro in human and mouse plasma and in vivo in the mouse. Role of the endothelium and the plasma proteinase inhibitors. J Clin Invest 1984;73:1696–703.
[16] Holton III OD, Black CD, Parker RJ, Covell DG, Barbet J, Sieber SM, et al. Biodistribution of monoclonal IgG1, F(ab0)2, and Fab0 in mice after intravenous injection. Comparison between anti-B cell (anti-Lyb8.2) and irrelevant (MOPC-21) antibodies. J Immunol 1987;139:3041–9.
[17] Schnitzer JE, Bravo J. High affinity binding, endocytosis, and degradation of conformationally modified albumins – potential role of gp30 and gp18 as novel scavenger receptors. J Biol Chem 1993;268:7562–70.
[18] Moestrup SK, Gliemann J, Pallesen G. Distribution of the alpha 2-macroglobin receptor/low density lipoprotein receptor-related protein in human tissues. Cell Tissue Res 1992;259:375–82.
[19] Lenting PJ, Neels JG, van den Berg BMM, van den Berg BMM, Clijsters PFM, Meijerman DWE, Pannekoek H, et al. The light chain of factor VIII comprises a binding site for low density lipoprotein receptor-related protein. J Biol Chem 1999;274:31305–11.
[20] Gopalakrishnan R, Hedner U, Ghosh S, Najak RC, Allen TC, Pendurthi UR, et al. Bio-distribution of pharmacologically administered recombinant factor VIIa (rFVIIa). Thromb Haemost 2010;8:301–10.
[21] Cheung WF, Hamaguchi N, Smith KJ, Stafford DW. Identification of the endothelial cell binding site for factor IX. Proc Natl Acad Sci U S A 1992;92:11068–73.
[22] Wolberg AS, Stafford DW, Erie DA. Human factor IX binds to specific sites on the collagenous domain of collagen IV. J Biol Chem 1997;272:16717–20.
[23] Gui T, Lin HF, Jin DY, Hoffman M, Straight DL, Roberts HR, et al. Circulating and binding characteristics of wild-type factor IX and certain Gla domain mutants in vivo. Blood 2002;100:153–8.
[24] Lindsay M. Characterization of post-translational modifications and resulting structure/function relationships of recombinant human factor IX produced in the milk of transgenic pigs. Chapter 5. Dissertation Blacksburg, VA: Virginia Polytechnic Institute and State University; 2004.
[25] Chaudhury C, Mehnaz S, Robinson JM, Hayton WL, Pearl DK, Roopenian DC, et al. The major histocompatibility complex-related Fc receptor for IgG (FcRn) binds albumin and prolongs its lifespan. J Exp Med 2003;197:315–22.
[26] Anderson CL, Chaudhury C, Kim J, Bronson CL, Wani MA, Mohanty S. Perspective – FcRn transports albumin: relevance to immunology and medicine. Trends Immunol 2006;27:343–8.
[27] Kim J, Bronson CL, Hayton WL, Radmacher MD, Roopenian DC, Robinson JM, et al. Albumin turnover: FcRn-mediated recycling saves as much albumin from degradation as the liver produces. Am J Physiol Gastrointest Liver Physiol 2005;290:G352–60.
[28] Kuo TT, Baker K, Yoshida M, Qiao SW, Aveson VG, Lencer WI, et al. Neonatal Fc receptor: from immunity to therapeutics. J Clin Immunol 2010;30:777–89.
[29] Roopenian DC, Sun VZ. Clinical ramifications of the MHC family Fc receptor FcRn. J Clin Immunol 2010;30:790–7.
[30] Siddiqui SS, Siddiqui ZK, Malik AB. Albumin endocytosis in endothelial cells induces TGF-beta receptor II signaling. Am J Physiol Lung Cell Mol Physiol 2004;286:L1016–26.
[31] Ghinea N, Eskenasy M, Simionescu M, Simionescu N. Endothelial albumin binding proteins are membrane-associated components exposed on the cell surface. J Biol Chem 1989;264:4755–8.
[32] Schnitzer JE, Carley WW, Palade GE. Albumin interacts specifically with a 60-kDa microvascular endothelial glycoprotein. Proc Natl Acad Sci U S A 1988;85:6773–7.
[33] Vogel SM, Minshall RD, Pillpovic M, Tiruppathi C, Malik AB. Albumin uptake and transcytosis in endothelial cells in vivo induced by albumin-binding protein. Am J Physiol Lung Cell Mol Physiol 2001;281:L1512–22.
[34] Thomsen MK, Diness V, Nilsson P, Rasmussen SN, Taylor T, Hedner U. Pharmacokinetics of recombinant factor VIIa in the rat. A comparison of bio-, immuno- and isotope assays. Thromb Haemost 1993;70:458–64.
[35] Termine JD, Kleinman HK, Whitson SW, Conn KM, McGarvey ML, Martin GR. Osteonectin, a bone-specific protein linking mineral to collagen. Cell 1981;26:99–105.
[36] Levick JR. Permeability of rheumatoid and normal human synovium to specific plasma proteins. Arthritis Rheum 1981;24:1550–60.
[37] Wunder A, Muller-Ladner U, Stelzer EH, Funk J, Neumann E, Stehle G, et al. Albumin-based drug delivery as novel therapeutic approach for rheumatoid arthritis. J Immunol 2003;170:4793–801.
[38] Yeh P, Landais D, Lemaitre M, Maury I, Crenne JY, Becquart J, et al. Design of yeast-secreted albumin derivatives for human therapy: biological and antiviral properties of a serum albumin-CD4 genetic conjugate. Proc Natl Acad Sci U S A 1992;89:1904–8.
[39] Kratz F. Albumin as a drug carrier: Design of prodrugs, drug conjugates and nanoparticles. J Control Release 2008;132:171–83.